Geoscience Frontiers 6 (2015) 617–625

HOSTED BY

Contents lists available at ScienceDirect

China University of Geosciences (Beijing)

Geoscience Frontiers

journal homepage: www.elsevier.com/locate/gsf

Research paper

Mesozoic and Cenozoic uplift and exhumation of the Bogda Mountain, NW China: Evidence from apatite fission track analysis

Wenhao Tang [a,b], Zhicheng Zhang [a,b,*], Jianfeng Li [a,b], Ke Li [a,b], Zhiwen Luo [a,b], Yan Chen [a,b]

[a] The Key Laboratory of Orogenic Belts and Crustal Evolution, Ministry of Education, Beijing 100871, China
[b] Department of Geology, School of Earth and Space Sciences, Peking University, Beijing 100871, China

ARTICLE INFO

Article history:
Received 13 September 2013
Received in revised form
19 March 2014
Accepted 17 April 2014
Available online 4 May 2014

Keywords:
Apatite fission track
Thermal history
Exhumation
Mesozoic–Cenozoic
Bogda Mountain

ABSTRACT

Apatite fission track (AFT) analysis on samples collected from a Paleozoic series is used to constrain the cooling history of the Bogda Mountain, northwest China. AFT ages range from 136.2 to 85.6 Ma and are younger than rock depositional ages and the mean confined track lengths (11.0–13.2 μm) mostly showing unimodal distribution are shorten, indicating significant track-annealing. Thermal histories modeling based on the distribution of fission-track lengths combined with the regional geological data show that two rapid cooling phases occurred in the latest Jurassic–early Cretaceous and the Oligocene–Miocene. Those new data together with previous published data show that the AFT ages become younger from the southwest to northeast in the western Bogda Mountain and its adjacent areas. The fission-track ages of the southwest area are relatively older (>100 Ma), recording the earlier rapid uplift phase during the late Jurassic–Cretaceous, while the ages in the north piedmont of the Bogda Mountain (namely the northeast part) are younger (<60 Ma), mainly reflecting the later rapid uplift phase in the Oligocene–Miocene. The trend of younger AFT ages towards the northeast might be explained by post-Cretaceous large-scale crustal tilting towards the southwest. In the thrust fault-dominated northern limbs of the Bogda Mountain, AFT ages reveal a discontinuous pattern with age-jumps across the major fault zones, showing a possible strata tilting across each thrust faults due to the thrust ramps during the Cenozoic. The two rapid uplift stages might be related to the accretion and collision in the southern margin of the Asian continent during the late Jurassic and late Cenozoic, respectively.

1. Introduction

The Tian Shan orogenic belt, one part of the Central Asian Orogenic Belt, is the result of two main tectonic events: complex arc-accretion, subduction and collision during the Paleozoic (Carroll et al., 1990, 1995; Allen et al., 1993; Sengör et al., 1993; Han et al., 2011; Xiao et al., 2012) and intracontinental reactivation and crustal shortening related to the ongoing India–Asia collision since the early Tertiary (Molnar and Tapponnier, 1975; Avouac et al., 1993; Yin, 2010). The present-day Chinese Tian Shan is one of the world's largest mountain ranges and can be divided into eastern and western segments roughly along the Wu-Ku road (from Urumqi to Korla, Fig. 1a).

In the eastern segment of the Chinese Tian Shan, the Bogda Mountain is situated between the Junggar Basin to the north and the Tu–Ha Basin to the south (Fig. 1a). The tectonic evolution of the Bogda Mountain since the Cenozoic India–Asia collision has been dominated by north–south compression. However, tectonic processes prior to the collision remain ambiguous. No agreement has been reached about the time of inception of the uplift and exhumation of the Bogda Mountain: the end of the Paleozoic (Wang et al., 2003), the early–middle Jurassic (Hendrix et al., 1992; Greene et al., 2001), or the late Jurassic (Zhang et al., 2005; Fang et al., 2007a). Even the processes causing the uplift and

* Corresponding author. Room 3307, Yifu-2 Building, Peking University, No. 5 Yiheyuan Road, Haidian District, Beijing 100871, China. Tel.: +86 10 62757287; fax: +86 10 62751159.
E-mail address: zczhang@pku.edu.cn (Z. Zhang).
Peer-review under responsibility of China University of Geosciences (Beijing)

1674-9871/$ – see front matter © 2015, China University of Geosciences (Beijing) and Peking University. Production and hosting by Elsevier B.V. All rights reserved.
http://dx.doi.org/10.1016/j.gsf.2014.04.006

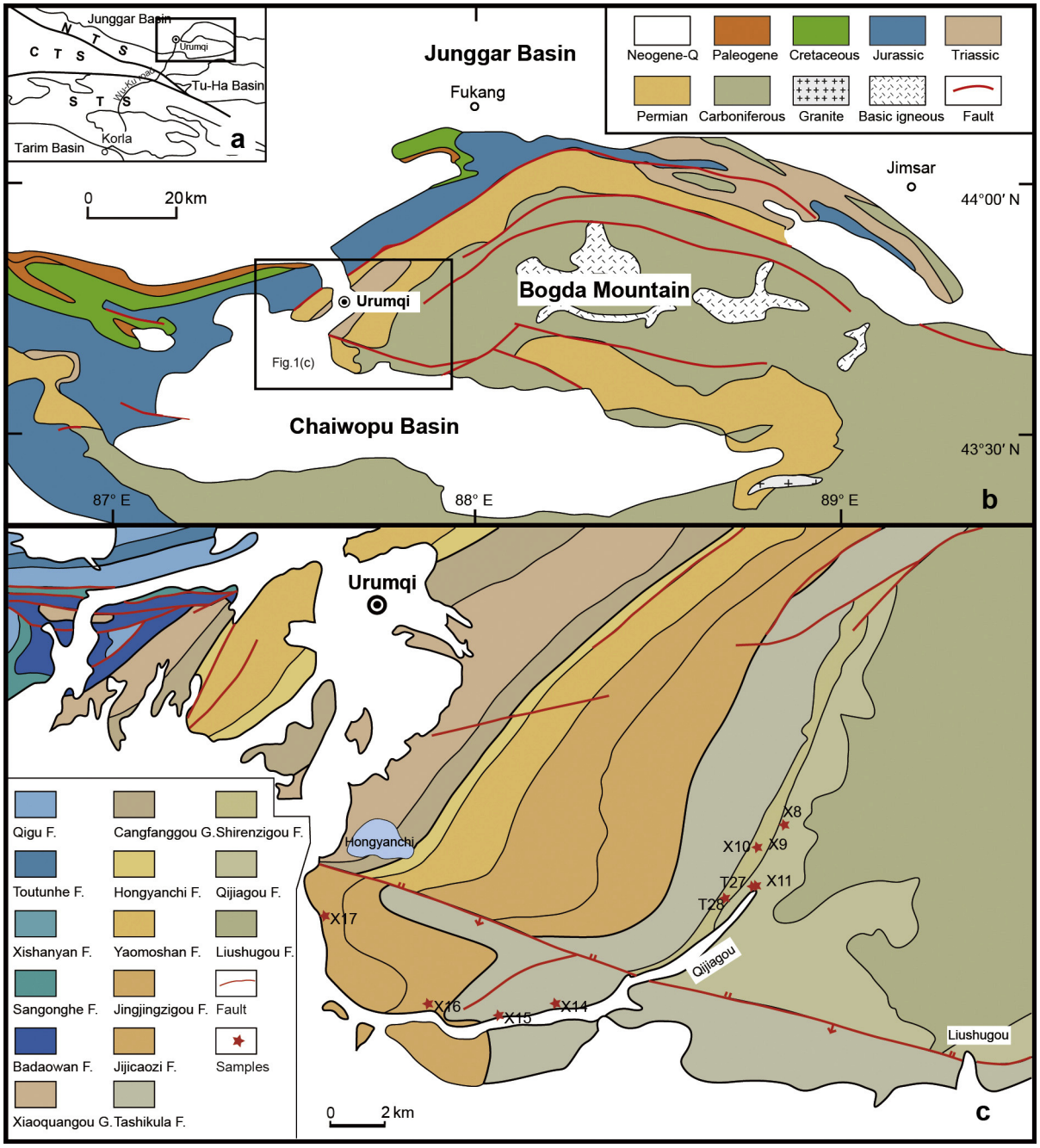

Figure 1. (a) Tectonic outline map of the Chinese Tian Shan. NTS – Northern Tian Shan; CTS – Central Tian Shan; STS – Southern Tian Shan (modified from Wang et al., 2007a). (b) Geological and tectonic sketch map of the Bogda Mountain (modified from Wang et al., 2007a). (c) Geological and tectonic sketch map of the west end of the Bogda Mountain with samples locations (modified from BGMRXUAR, 1993).

exhumation of the Bogda Mountain are debated. Previous studies indicate that the Bogda areas have experienced several periods of uplift and exhumation since the Mesozoic, mainly including the latest Jurassic (about 150 Ma), the early Cretaceous (about 100 Ma), the latest Cretaceous (about 65 Ma), the middle Eocene (about 40 Ma), the early Miocene (about 20 Ma) and the latest Miocene (about 10 Ma) (Shen et al., 2005, 2008; Zhu et al., 2006; Wang et al., 2007a, 2008).

Apatite fission-track (AFT) analysis can be used to obtain information about cooling history and exhumation of rocks. This paper presents the results that new data yield on the Mesozoic and Cenozoic thermal history and provides a new interpretation model of the tectonic evolution of the Bogda Mountain and its adjacent areas.

2. Geological setting and stratigraphy characteristics

The Bogda Mountain is an east–west trending and northward prominent arcuated mountain. It is a box anticline mainly composed of marine volcanic rocks, pyroclastic rocks and carbonate rocks formed in the middle and upper Carboniferous (Allen et al., 1993; Li, 2004). There are few syntectonic granites and low-grade (greenschist facies) metamorphic rocks (Ma et al., 1993). Because of N–S compression, a series of thrust faults developed in the north

piedmont of the Bogda Mountain (Fig. 1b). The arc-shaped south-dipping thrust faults and folded cover strata constitute the transition zone between the Bogda Mountain and the Junggar Basin (Li et al., 2004). In the study area, the thrust belt is cut by a transpressional dextral fault along Hongyanchi–Liushugou lineament (BGMRXUAR, 1993; Fig. 1c).

Carboniferous and Permian strata, as well as a small amount of Triassic and Jurassic strata to the north, are well-preserved and exposed in the west end of the Bogda Mountain (BGMRXUAR, 1993, 2008). The middle Carboniferous series consist of the Liushugou Formation and the Qijiagou Formation, which are mainly composed of andesitic volcanic breccia, agglomerate, tuff, carbonates and minor sandstone lenses. The upper Carboniferous series consist of the Shirenzigou Formation and the Tashikula Formation, which are composed of arkose, siltstone and limestone lenses. The depositional environments evolved from a shallow marine system in the middle Carboniferous to a coastal system in the late Carboniferous.

The Permian series can be divided into the Jijicaozi Formation, the Jingjingzigou Formation, the Yaomoshan Formation and the Hongyanchi Formation, which are mainly terrigenous clastic strata. The sediments are composed of gray-green siltstone, dolomitic limestone, tuff, sandstone, shale, oil shale, and small quantities of limestone.

The Triassic series, lying conformably on the Permian series, consist of the Cangfanggou Group and the Xiaoquangou Group. The sediments are composed of brown-gray-colored mudstones, argillaceous siltstones, litharenites, and sandy mudstones. The Cangfanggou Group is characterized by typical braided river to deltaic sandy conglomerates (Wu et al., 2006).

The Jurassic series, showing a maximum thickness over 4000 m, are widely distributed in the Junggar Basin, Tarim Basin and Tu–Ha Basin. The sequences can be divided into the lower Jurassic Badaowan Formation and Sangonghe Formation, the middle Jurassic Xishanyao Formation and Toutunhe Formation, and the upper Jurassic Qigu Formation and Kalazha Formation. The lower and middle Jurassic series are mainly composed of gray-green sandstones and mudstones rich in coal layers and coal streaks which can be regarded as the characteristics of lake swamp deposition. The upper Jurassic Qigu Formation is characterized by brown-purple mudstones, sandstones and thin-bedded tuff whereas the Kalazha Formation is formed by a typical brown-reddish thick-bedded conglomerate, indicating a large alluvial fan deposition environment.

The Cretaceous series are not exposed in the study area. In the neighbor Toutunhe area, they lay unconformably on the Jurassic series, and are mainly composed of gray-green mudstones and sandstones interbedded with conglomerates. The Cenozoic series mainly consist of sandstones, mudstones and conglomerates.

The magmatism of the Bogda area is not active since the late Permian. There are some outcrops of the Carboniferous basic-mafic igneous rocks near the Bogda Peak and granite in the eastern Chaiwopu Basin (Fig. 1b). In our study area, there is only limited amount of the Variscan granodiorite porphyry and quartz diorite porphyry intruded in the Carboniferous series.

3. Sampling and analytical method

Ten rock samples ranging in ages from the late Carboniferous to the early Permian were collected from the Qijiagou field section in the western piedmont of the Bogda Mountain (Fig. 1c). Nine of the samples are medium-grained to coarse-grained sandstones, and the other one is a diorite porphyry. The location information of the samples, including altitude, latitude and longitude coordinates, was obtained by the portable GPS. Their altitude is from 1017 to 1343 m (Table 1).

Table 1
Geographic position and lithology of the samples.

Sample	Altitude (m)	Latitude	Longitude	Lithology and depositional age
X8	1343	43°42′58″	87°48′07″	Tuffaceous sandstone containing gravel; C_2
X9	1326	43°42′29″	87°47′34″	Diorite porphyry intrusive in Carboniferous series
X10	1326	43°42′29″	87°47′34″	Gray-green sandstone; C_3
X11	1269	43°41′38″	87°47′16″	Gray pebbly coarse sandstone; C_2
T27	1277	43°41′37″	87°47′15″	Gray-green sandstone; C_2
T28	1283	43°41′23″	87°46′24″	Off-white coarse sandstone; C_3
X14	1124	43°39′17″	87°41′26″	Gray pebbly coarse sandstone; C_3
X15	1096	43°39′06″	87°39′46″	Gray coarse sandstone; C_3
X16	1076	43°39′18″	87°38′11″	Gray coarse sandstone; P_1
X17	1017	43°41′12″	87°35′28″	Gray-green fine sandstone; P_1

Fission tracks are damaged zones of the crystal lattice caused by the spontaneous nuclear fission of ^{238}U at a constant rate. In apatite, fission tracks form with a constant initial length of about 16.3 μm (Gleadow and Duddy, 1981; Gleadow et al., 1986a,b). Fission tracks will anneal, or shorten inevitably, when the host mineral is at an elevated temperature. Significant annealing of apatite fission tracks occurs in a temperature interval between ~60 and 110 ± 10 °C in geological time scales, the temperature range termed the partial annealing zone (PAZ) (Gleadow et al., 1986a; Green et al., 1989; Fitzgerald and Gleadow, 1990). Therefore, the confined track-length distribution is a sensitive monitor of a thermal history of a rock sample. AFT analysis can provide detailed information on the low-temperature thermal history and exhumation of rocks (Gallagher et al., 1998; Dumitru et al., 2001).

The apatite crystals were separated from bulk rock samples following the standard procedures used for mineral separation. This work was conducted by the Chengxin Geology Service Co. Ltd, Langfang, Hebei Province, China. AFT ages were determined using the external detector method (Hurford and Green, 1983). The experimental samples were prepared and analyzed at the Fission Track Lab of the Key Laboratory of Orogenic Belts and Crustal Evolution, Ministry of Education in Peking University. The apatite grains were glued with epoxy on glass slides, grounded and polished to expose the mineral maximum inner surface, and then etched in 5 N HNO_3 for 20 s at room temperature, in order to reveal spontaneous fission tracks (Li et al., 2010). Grain mounts and Corning CN5 glass dosimeters were packed together with low-uranium muscovite external detectors and irradiated with thermal neutrons at a nuclear reactor of the China Institute of Atomic Energy, with a nominal neutron flux of 1.0×10^{16} n/cm^2. After irradiation the mica external detectors were etched in 40% HF for 20 min at room temperature to reveal induced fission tracks. The ages were calculated using the zeta (ζ) calibration method (Hurford and Green, 1983) recommended by the Fission Track Working Group of the International Union of Geological Sciences Subcommission on Geochronology (Hurford, 1990). The zeta value is 384.01 ± 11.17, obtained from Durango (McDowell et al., 2005) and Fish Canyon Tuff (Naeser and Cebula, 1985) standards. Fission tracks were counted on a Zeiss microscope, using a magnification of 1000 × under dry objectives. Confined tracks were measured using the Autoscan system.

4. Results and thermal history modeling

Ten samples were analyzed. AFT data are shown in Table 2. The P (χ^2) of all samples is greater than 5%, indicating that the single-grain ages belong to the same age group (Green, 1981). The sample mean age is expressed by the pooled age. Because of the small size of apatite crystals, the analyzed area of each apatite grain is

Table 2
AFT data of the samples from the Bogda Mountain.

Sample	N	ρ_d (10^5/cm^2)	N_d	ρ_s (10^5/cm^2)	N_s	ρ_i(10^5/cm^2)	N_i	P (%)	Pooled (Ma)	($\pm1\sigma$)	L (μm)	St. D	N	Dpar (μm)	N
X8	12	12.604	7960	2.477	32	5.138	64	99.7	119.9	26.2	13.0	1.3	2	2.16	32
X9	23	12.473	7960	2.917	59	5.241	106	100.0	131.9	21.9	11.5	1.3	6	2.39	54
X10	17	12.209	7960	3.451	38	5.773	60	100.0	136.2	28.6	11.0	2.8	13	2.99	41
X11	6	12.341	7960	2.815	10	5.511	21	98.5	119.9	43.1	11.1	3.1	3	4.09	10
T27	15	11.484	7653	3.449	35	6.08	63	100.0	121.3	25.9	11.2	2.3	22	2.04	26
T28	22	11.611	7653	5.378	121	9.467	213	100.0	125.4	14.8	11.1	2.4	23	1.69	50
X14	21	11.666	6854	5.018	167	10.787	359	92.6	103.4	10.2	12.3	1.9	86	2.7	54
X15	24	11.549	6854	4.935	155	9.934	312	100.0	109.2	11.3	13.2	1.5	85	2.85	92
X16	23	11.433	6854	3.545	108	9.026	275	99.8	85.6	10.1	11.9	2.3	20	2.45	60
X17	22	11.316	6854	4.712	118	9.606	249	87.1	102.2	11.9	12.4	1.6	88	2.27	95

N – the number of grains; ρ_d – the density of induced fission track ($\times10^5$/cm^2) that would be obtained in each sample if its U concentration was equal to the U concentration of the CN5 glass dosimeter; N_d – numbers in parentheses are total numbers of tracks counted; ρ_s – the spontaneous track density ($\times10^5$/cm^2); N_s – the spontaneous track number; ρ_i – the induced track density ($\times10^5$/cm^2); N_i – the induced track number; P (%) – the probability of χ^2; L – the average length of confined tracks; ζ_{CN5}=384.01 ± 11.17.

small, resulting in few counted spontaneous tracks (N_s). The ages range from 136.2 to 85.6 Ma, and the track lengths range from 11.0 to 13.2 μm, with standard deviations between 1.3 and 3.1 μm (Table 2 and Fig. 2).

4.1. Fission track results

AFT single-grain ages are far younger than the late Caboniferous to early Permian sample stratigraphic ages (radial plot, Fig. 2) indicating that the apatites were reset at least once after being deposited. The confined track lengths are shorter than the fission-track initial length (16.3 μm), showing unimodal distribution. The characteristics of fission-track lengths indicate that the apatite of samples in the west end of the Bogda Mountain had experienced a significant annealing. The shortened track lengths suggest that the samples spent quite a long time in the PAZ after reset. Relatively old fission-track ages indicate that the samples entered in the PAZ relatively early, as demonstrated by subsequent results of thermal history modeling. The AFT ages show a positive correlation with the altitude, whereas, on the contrary, the AFT lengths show a negative correlation (Fig. 3a). The pattern of the AFT data on the two sides of the Hongyanchi–Liushugou fault is slightly different (Fig. 3a): AFT ages are generally younger (109.2–85.6 Ma), and the lengths are longer (average about 12.5 μm) on the hanging wall; on the foot-wall, the AFT ages are older (136.2–119.9 Ma), and the lengths are shorter (mainly about 11 μm). Taking into account the altitude differences, such age differences may be just because samples at higher altitudes cooled earlier.

4.2. Thermal history modeling

An AFT age may represent a complex history of past thermal events. Except the case of rapid cooling from temperatures higher than the PAZ in which the AFT age correspond to the time of cooling, usually the AFT age has not a simple geological meaning (Zhang and Wang, 2004). AFT ages and the length distribution can be combined together using various modeling procedures in order to investigate the possible thermal histories of the rock sample (Jolivet et al., 2001). Because AFTs are immediately annealed at temperature higher than 110 ± 10 °C and annealed very slowly at temperatures lower than 60 °C ("immediately" and "slowly" refer to geologically significant rates of the order of the Ma), track length modeling can describe the T–t evolution of the sample between 110 and 60 °C (Corrigan, 1991; Jolivet et al., 2010). In this work, thermal history modeling was done using the HeFTy software (Ketcham, 2005) with the annealing model of Ketcham et al. (2007) that takes into account the Dpar and the angle with C-axis parameters. Only samples with at least 50 track-length measurements were modeled.

An inverse modeling procedure was performed with the following constraints: (1) the starting time was constrained by the deposition ages of the rock samples and assuming that the surface temperature of the Junggar Basin in the Paleozoic was of about 15 °C (Pan et al., 1997); (2) the end of the time-temperature paths was set at 7.5 °C according to the present-day annual average temperature (Li et al., 2012). The geothermal gradient of the Junggar Basin was 43.3–50 °C/km in the Carboniferous and reduced to about 30 °C/km in the Mesozoic, and the geothermal gradient of present now is 22.8 °C/km (Qiu et al., 2002). The magmatism has not been active since late Permian in the study area. Therefore, the increase of paleotemperature was primarily due to the sediments burial, while the decrease of it was caused by the uplift and exhumation.

Thermal modeling of the AFT data was performed only on samples where enough track lengths could be measured. Results of thermal modeling for three samples (X14, X15 and X17) show that they all experienced two remarkably rapid cooling phases: latest Jurassic (about 150 Ma) and Miocene (about 20 Ma)(Fig. 4). From the thermal modeling, it results that samples were heated at temperature higher than the bottom of the PAZ and were completely reset in the latest Jurassic. This is in agreement with the sedimentary record showing a thickness of about 5–7 km from late Paleozoic to late Jurassic. From 100 to 20 Ma, the thermal modeling shows a slow cooling process leaving the samples for a long time within the partial annealing zone. The increase of cooling rates since 20 Ma indicates a rapid exhumation at the west end of the Bogda Mountain since Miocene.

5. Discussion

5.1. The earlier cooling phase

The first cooling phase shown in thermal modeling indicates a rapid exhumation event in latest Jurassic, and it finds a confirmation in some geological evidences. The thick lacustrine coal-bearing strata of the early–middle Jurassic on both sides of the Bogda Mountain and the lower–middle Jurassic strata in the Bogda Mountain all indicate that the Bogda Mountain was still flooded as a depositional area accepting sediments, which is also in agreement with the paleocurrent and deposition diffusion style of the early–middle Jurassic directed towards the Bogda Mountain (Fang et al., 2006; Wang et al., 2007b). The upper Jurassic succession, divided into the Qigu Formation and the Kalazha Formation, is a coarsening-upward sequence from the brown-purple mudstones and sandstones in the bottom to the brown-reddish thick-bedded conglomerate in the top. The Cretaceous strata are not exposed in this study area, whereas the Cretaceous series cover the Jurassic series unconformably in the adjacent regions (BGMRXUAR, 1993,

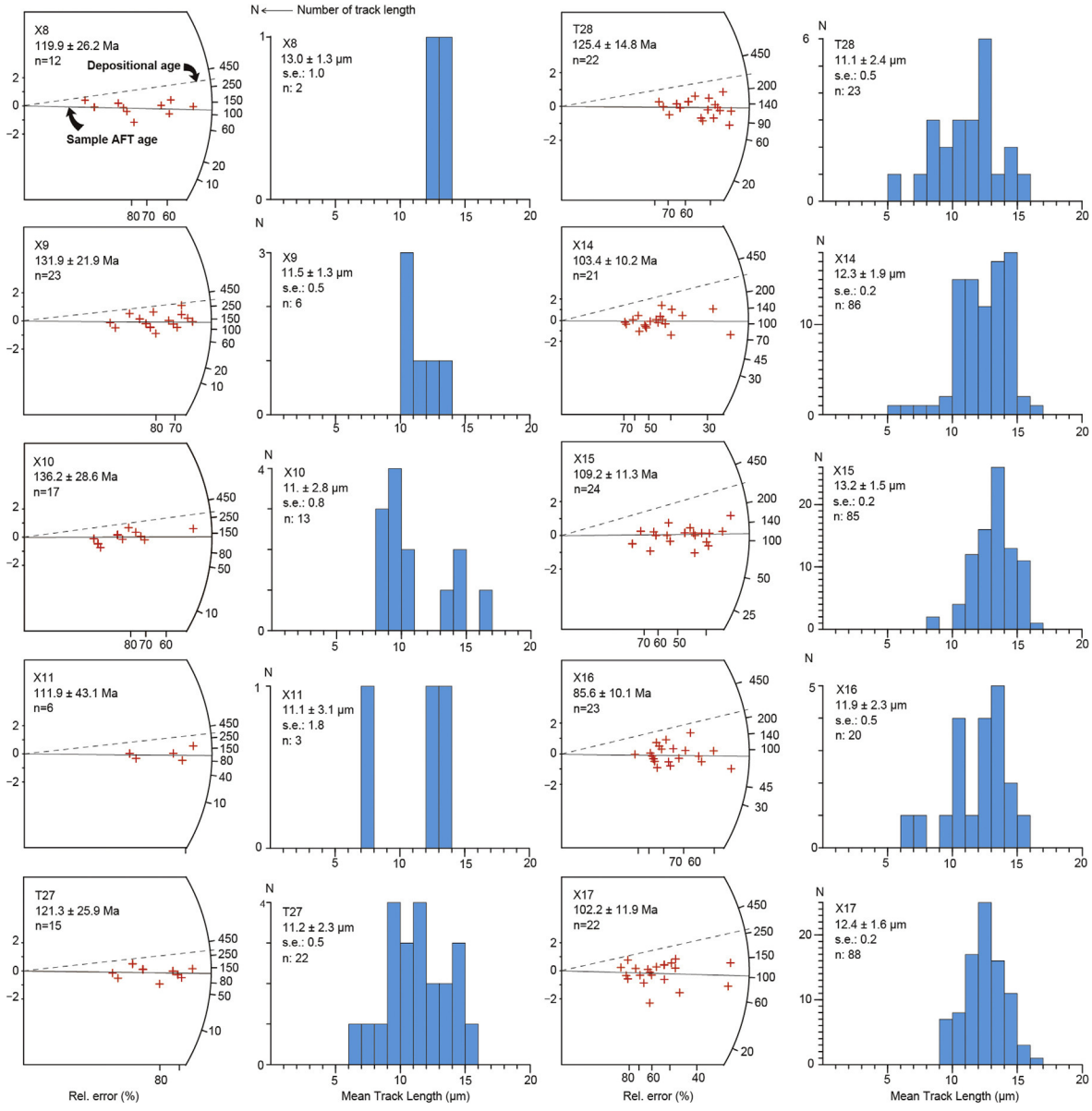

Figure 2. Radial plots of AFT single grain ages and track length histograms for samples at the west end of the Bogda Mountain (all ages are pooled ages).

2008). Stratigraphy and the seismic profiles CWP-588 and NS01 on both sides of the Bogda Mountain indicate that the angular unconformity between the pre-Cretaceous and Cretaceous strata is the first regional unconformity since the late Paleozoic (Zhang et al., 2005). In the southern margin of the Junggar Basin, Wang and Gao (2012) and Wang et al. (2012) studied the Jurassic–Cretaceous biostratigraphy and obtained a SHRIMP U-Pb zircon age of 164.6 ± 1.4 Ma (MSWD = 1.3) for tuff from so-called upper series of

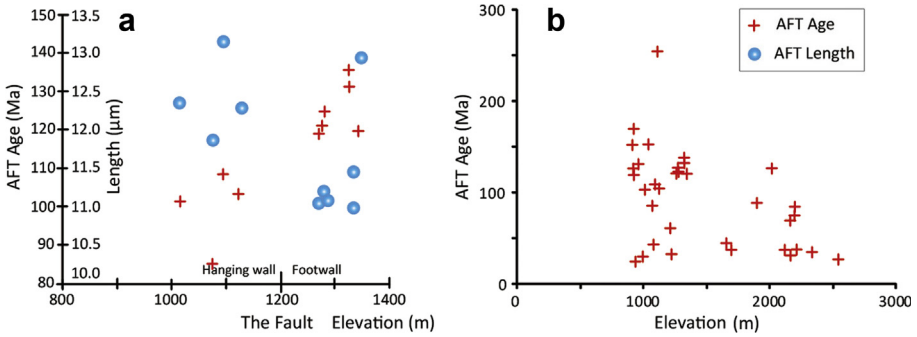

Figure 3. Relationship between elevation and fission track data of the Bogda Mountain. (a) Plot of AFT ages and confined track lengths versus the altitude on the two sides of the oblique-slip fault. (b) Plot of AFT ages versus the altitude in the Bogda Mountain and its adjacent areas (age data are from Shen et al., 2005; Guo et al., 2006; Zhu et al., 2006 and this study).

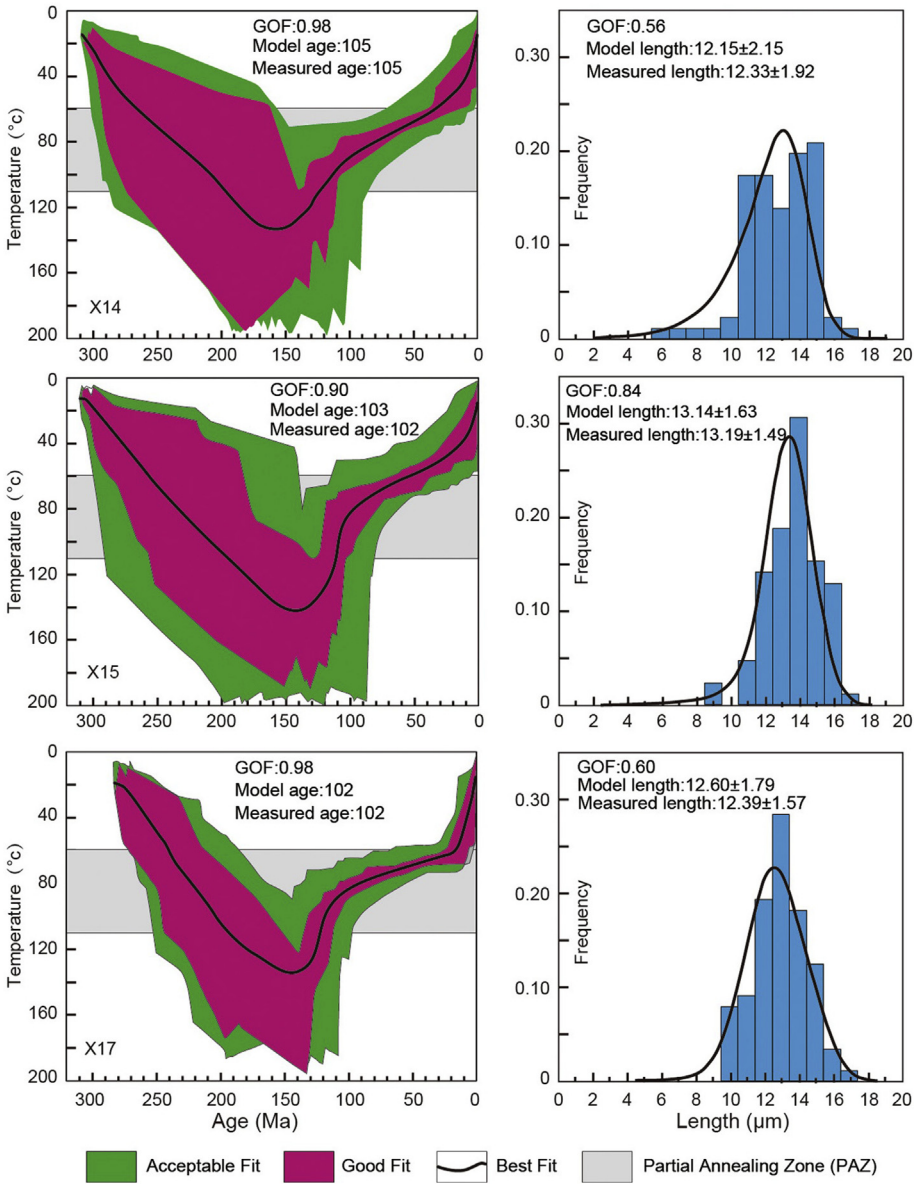

Figure 4. Temperature-time paths of thermal modeling and the length patterns for representative samples of the Bogda Mountain. GOF – Goodness of fit (0–1), a description of how well a statistical model fits a set of observations.

Jurassic Qigu Formation. They further speculated that this age corresponds broadly to the unconformity between the Jurassic and the Cretaceous and, together with the absence of the whole upper Jurassic, suggest that there was a strong tectonic movement in the late Jurassic. This tectonic uplift was confirmed by the analysis of detrital zircon geochronology in the southern margin of Junggar Basin (Li and Peng, 2013; Yang et al., 2013). An extensive record of the early Cretaceous rapid cooling was reported from the Tian Shan to the Tarim Basin (Guo et al., 2002; Zhang et al., 2007; Xiang et al., 2013).

The cooling rate was lower during the late Cretaceous. The decreased exhumation rate may be caused by absence of relevant tectonics. In other words, the study region shifted from a tectonic exhumation regime to an erosional regime. The upper Cretaceous to Paleogene series of the adjacent areas are characterized by fine sedimentary particles, like reddish siltstones, sandy mudstones and mudstones, which also indicate a lower deposition rate (BGMRXUAR, 1993, 2008; Li and Peng, 2013). This is consistent with that a peneplain formed with the erosional phase after the Cretaceous uplift (Zhang and Wu, 1985; Ma et al., 1993).

5.2. The later cooling phase

Geological records have confirmed that the later rapid cooling phase was caused by tectonic uplift in the Miocene. The growth strata included in the Miocene sedimentary strata of the Toutunhe area indicate tectonic uplift since the Miocene (Guo et al., 2006). The growth strata were also suggested by the seismic profiles in the southern margin of the Junggar Basin (Fang et al., 2007b). In the southern margin of the Junggar Basin, the Oligocene series mainly consist of mottled mudstones interbedded with sandstones, which are characteristic of lacustrine environments (Fang et al., 2006; Charreau et al., 2008). The Miocene series are mainly composed of brown-reddish sandy conglomerates and pelitic sandstones deposited in an alluvial plain environment (Guo et al., 2011; Yang et al., 2013). The coarsening-upward of the clastic sediments and

the evolution direction of the depositional system both suggest a surface uplift event during the Oligocene–early Miocene.

This rapid uplift event has been reported throughout the Tian Shan region (Dumitru et al., 2001; Guo et al., 2006; Zhang et al., 2007). AFT data indicate that the Mesozoic strata exposed on the northern flank of the Chinese Tian Shan underwent ~4–5 km of late Cenozoic unroofing, beginning at about 24 Ma (Hendrix et al., 1994). In the northern margin of the Tarim Basin, south Tian Shan, the AFT analysis for the granites and rhyolites suggested that there was a rapid uplift between 25 and 17 Ma and the uplift rate reached 138.8–198.8 m/Myr (Yang et al., 2003). According to the sedimentary stratigraphic sequences and the sandstones debris of the late Mesozoic–Cenozoic, Liu et al. (2004) agreed with the rapid uplift in the early Miocene (about 24 Ma) in the eastern Tian Shan. Similarly, data from the west Tian Shan also showed the rapid cooling process since Cenozoic (Sobel and Dumitru, 1997; Chen et al., 2006, 2008). The widespread tectonic uplift may be associated with the collision of the Indian plate since the late Cenozoic at the southern margin of the Asian continent (Tapponnier and Molnar, 1979; Jolivet et al., 2010).

5.3. Conceptual model of evolution

The distribution of AFT ages in the Bogda Mountain and its adjacent areas shows that ages become younger from the southwest to northeast (Fig. 5a), but the study area can be roughly divided into two parts by the Urumqi city. In the southwest part, the fission track ages are older, most of them are more than 100 Ma, while in the northeast area, scilicet on the north piedmont of the Bogda Mountain, the ages are younger, mainly less than 60 Ma. The older ages in the Toutunhe area to the southwest likely record the earlier uplift phase during the late Jurassic–early Cretaceous. The younger ages in the Fukang area to the northeast mainly reflect the later uplift phase in the Oligocene–Miocene. The AFT age–elevation plot based on all available data for the study region suggests that no obvious linear correlation exists between age and elevation (Fig. 3b). The distribution of AFT ages from the southwest to the northeast might be related to a post-Cretaceous large-scale crustal tilting towards the southwest.

In the north piedmont of the Bogda Mountain, there are several major thrust faults with similar occurrences (Fig. 1b) and a series of small faults (Li et al., 2004). The best constraint for the time of thrusting is given by the AFT ages on the hangingwall of each thrust. Along the cross section (Fig. 5b), it is quite clear that ages close to the fault (on the hangingwall side) are all between about 25 and 30 Ma, whereas, on the footwall, they are much older. This means that age of thrusting was at least at 25–30 Ma or a few million years younger. This is consistent with the geological observation in the field. Mesozoic strata northward thrust over the Cenozoic strata and form drag folds in the leading edge of fold-thrust belt, which indicates the strong thrust activity in the Cenozoic (Chen et al., 2012). Creation of structural high due to thrusting in Cenozoic may have enhanced rock exhumation in the northeast part (the Fukang area) bring to exposure younger AFT ages.

A cross-section across the west end of the Bogda Mountain shows a simplified conceptual model of the AFT age stratigraphy (Fig. 5b). All sedimentary stratigraphy and geological structures are ignored except the main thrust faults. The north piedmont of the Bogda Mountain is divided into several blocks by the main thrust faults (Fig. 1b). The AFT ages on each block gradually become younger northward. It implies that the AFT age stratigraphy was tilted owing to the thrust faults. The youngest age (about 10 Ma) on

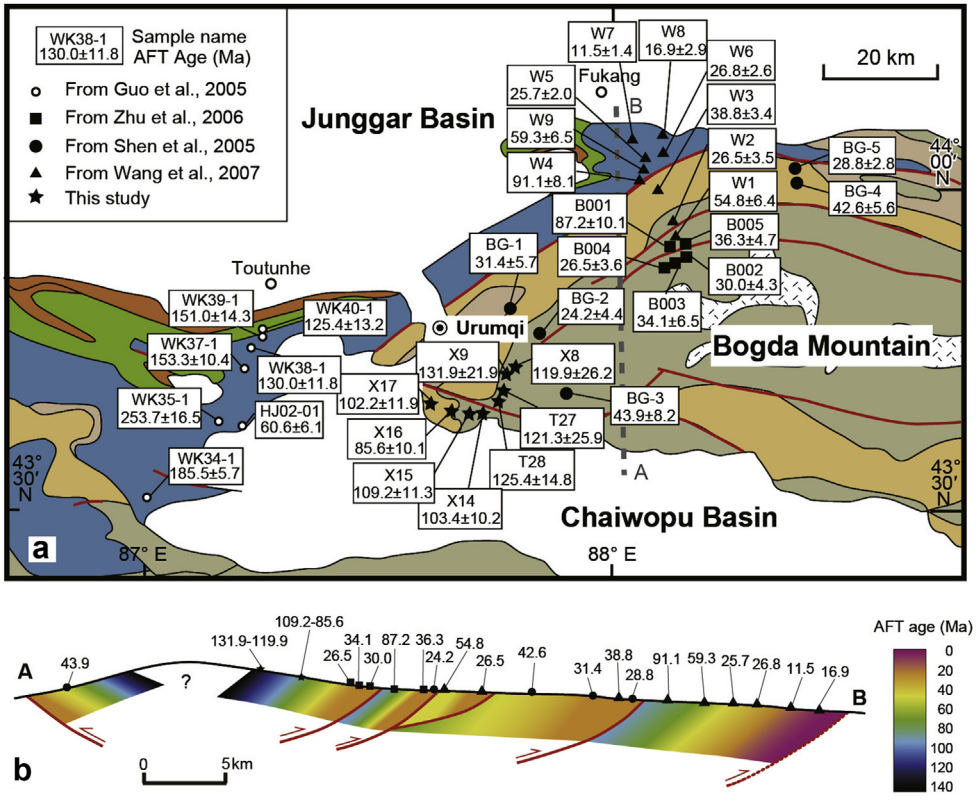

Figure 5. The characteristics of AFT ages in the Bogda Mountain and its adjacent areas. (a) The distribution of AFT ages in the study region (the ages are from Shen et al., 2005; Guo et al., 2006; Zhu et al., 2006; Wang et al., 2007a and this study). (b) Simplified conceptual model across the west end of the Bogda Mountain. The section displays only the AFT age stratigraphy and the main thrust faults. All sedimentary stratigraphy and structures are ignored. Dashed line represents the buried thrust fault.

the northernmost block suggest the latest possible tectonic activity occurred during the late Miocene. The AFT ages in the cross-section likely become younger from south to north, which might imply that the thrusting with the related uplift and exhumation expanded northward (Wang et al., 2007a). This is consistent with the widespread tectonic uplift in northwest China associated with the Indian–Asian collision since the late Cenozoic.

6. Conclusions

Single-grain AFT ages from sample from western Bogda Mountains region are much younger than their depositional ages and the mean confined track lengths (11.0–13.2 μm) are shorter than the initial track length (16.3 μm), which indicate the reset of the AFT system and a subsequent slow cooling through the PAZ.

The time–temperature histories modeling based on the distribution of fission track lengths show that the Bogda Mountain has experienced two rapid uplift and exhumation phases: the latest Jurassic–early Cretaceous and the Oligocene–Miocene. The two rapid uplift stages might be associated with the accretion of the Lhasa Block in the late Jurassic and the collision of the Indian plate since the late Cenozoic at the southern margin of the Asian continent, respectively.

In the western Bogda Mountain and its adjacent areas, the AFT ages become younger from the southwest to northeast. The AFT ages of the southwest area are much older (>100 Ma), reflecting the earlier rapid uplift phase during the late Jurassic–Cretaceous, while the ages in the north margin of the Bogda Mountain (namely the northeast part) are younger (<60 Ma), mainly recording the later rapid uplift phase in the Cenozoic. The trend of younger AFT ages towards the northeast may be explained by post-Cretaceous large-scale crustal tilting towards the southwest. In the fault-dominated northern limbs of the Bogda Mountain, AFT ages on each block gradually become younger northward, showing a possible strata tilting across each thrust faults due to the thrust ramps during the Cenozoic.

Acknowledgments

We are indebted to Massimiliano Zattin and another anonymous reviewers for their detailed comments and constructive suggestions, which greatly improved the original draft of the manuscript. This work was supported by the State Science and Technology Major Project (2009ZX05009-001).

References

Allen, M.B., Windley, B.F., Zhang, C., 1993. Palaeozoic collisional tectonics and magmatism of the Chinese Tien Shan, central Asia. Tectonophysics 220, 89–115.

Avouac, J.P., Tapponnier, P., Bai, M., You, H., Wang, G., 1993. Active thrusting and folding along the northern Tien-shan and late Cenozoic rotation of the Tarim relative to Dzungaria and Kazakhstan. Journal of Geophysical Research-Solid Earth 98, 6755–6804.

BGMRXUAR (Bureau of Geology and Mineral Resources of Xinjiang Uygur Autonomous Region), 1993. Regional Geology of Xinjiang Uygyr Autonomous Region. Geological Publishing House, Beijing, pp. 136–227 (in Chinese).

BGMRXUAR (Bureau of Geology and Mineral Resources of Xinjiang Uygur Autonomous Region), 2008. The Research on the Nationwide Multifold Stratigraphic Division and Correlation the Lithostratigraphy of Xinjiang Uygur Autonomous Region. China University of Geosciences Press, Wuhan, pp. 55–120 (in Chinese).

Carroll, A.R., Graham, S.A., Hendrix, M.S., Ying, D., Zhou, D., 1995. Late Paleozoic tectonic amalgamation of northwestern China: sedimentary record of the northern Tarim, northwestern Turpan, and southern Junggar Basins. Geological Society of America Bulletin 107, 571–594.

Carroll, A.R., Liang, Y., Graham, S.A., Xiao, X., Hendrix, M.S., Chu, J.C., Mcknight, C.L., 1990. Junggar Basin, northwest China: trapped late Paleozoic ocean. Tectonophysics 181, 1–14.

Charreau, J., Avouac, J.P., Chen, Y., Dominguez, S., Gilder, S., 2008. Miocene to present kinematics of fault-bend folding across the Huerguosi anticline, northern Tianshan (China), derived from structural, seismic, and magnetostratigraphic data. Geology 36, 871–874.

Chen, K., Wang, Z.Y., Liu, F., Jiang, L., Lin, W., Wang, Q.C., 2012. The structural characteristics along the northern piedmont of Bogedashan and its dynamic significances. Chinese Journal of Geology 47, 1041–1051 (in Chinese with English abstract).

Chen, Z.L., Wan, J.L., Liu, J., Li, S.X., Zheng, E.J., Han, X.Z., Li, X.G., Gong, H.L., 2006. Multi-stage uplift and exhumation of the West Tianshan Mountain: evidence from the apatite fission-track dating. Acta Geoscientica Sinica 27, 97–106 (in Chinese with English abstract).

Chen, Z.L., Li, L., Liu, J., Gong, H.L., Jiang, R.B., Li, S.X., Zheng, A.J., Han, X.Z., Li, X.G., Wang, C., Wang, G.R., Wang, G., Lu, K.G., 2008. Preliminary study on the uplifting-exhumation process of the western Tianshan range, northwestern China. Acta Petrologica Sinica 24, 625–636 (in Chinese with English abstract).

Corrigan, J., 1991. Inversion of apatite fission track data for thermal history information. Journal of Geophysical Research 96, 10347–10360.

Dumitru, T.A., Zhou, D., Chang, E.Z., Graham, S.A., 2001. Uplift, exhumation, and deformation in the Chinese Tian Shan. In: Hendrix, M.S., Davis, G.A. (Eds.), Paleozoic and Mesozoic tectonic evolution of central Asia: From continental assembly to intracontinental deformation, Geological Society of America Memoir 194, pp. 71–99.

Fang, S.H., Guo, Z.J., Wu, C.D., Zhang, Z.C., Wang, M.N., 2006. Jurassic clastic composition in the Southern Junggar Basin, Northwest China: Implications for basin-rang pattern and tectonic attributes. Acta Geological Sinica 80, 196–209 (in Chinese with English abstract).

Fang, S.H., Song, Y., Jia, C.Z., Wang, X.L., Yuan, Q.D., 2007a. The Mesozoic-Cenozoic clastic composition of Bogda area, Xinjiang: Implications on the evolution of basin-range pattern. Acta Geologica Sinica 81, 1229–1236 (in Chinese with English abstract).

Fang, S.H., Song, Y., Jia, C.Z., Guo, Z.J., Zhang, Z.C., Liu, L.J., 2007b. Timing of Cenozoic intense deformation at the north margin of Tianshan and its implications for petroleum arccumulation. Earth Science Frontiers 14, 205–214 (in Chinese with English abstract).

Fitzgerald, P.G., Gleadow, A.J.W., 1990. New approaches in fission track geochronology as a tectonic tool: examples from the Transantrarctic mountains. Nuclear Tracks and Radiation Measurements 17, 351–357.

Gallagher, K., Brown, R., Johnson, C., 1998. Fission track analysis and its applications to geological problems. Annual Review of Earth and Planetary Sciences 26, 519–572.

Gleadow, A.J.W., Duddy, I.R., 1981. A natural long-term track annealing experiment for apatite. Nuclear Tracks and Radiation Measurements 5, 169–174.

Gleadow, A.J.W., Duddy, I.R., Green, P.F., Hegarty, K.A., 1986a. Fission track lengths in the apatite annealing zone and the interpretation of mixed ages. Earth and Planetary Science Letters 78, 245–254.

Gleadow, A.J.W., Duddy, I.R., Green, P.F., Lovering, J.F., 1986b. Confined fission track lengths in apatite – a diagnostic tool for thermal history analysis. Contributions to Mineralogy and Petrology 94, 405–415.

Green, P.F., 1981. A new look at statistics in fission-track dating. Nuclear Tracks and Radiation Measurements 5, 77–86.

Green, P.F., Duddy, I.R., Gleadow, A.J.W., Lovering, J.F., 1989. Apatite fission-track analysis as a paleotemperature indicator for hydrocarbon exploration. In: Naeser, N.D., McCulloch, T.H. (Eds.), Thermal History of Sedimentary Basins: Methods and Case Histories. Springer, New York, pp. 181–195.

Greene, T.J., Carroll, A.R., Hendrix, M.S., Graham, S.A., Wartes, M.A., Abbink, O.A., 2001. Sedimentary record of Mesozoic deformation and inception of the Turpan-Hami basin, northwest China. Geological Society of America 194, 317–340.

Guo, Z.J., Zhang, Z.C., Liao, G.H., Fang, S.H., 2002. Uplifting process of eastern Tianshan Mountains: evidence from fission-track age and its tectonic significance. Xingjiang Geology 4, 331–334 (in Chinese with English abstract).

Guo, Z.J., Fang, S.H., Zhang, R., Zhang, Z.C., Wu, C.D., Shao, K.Z., 2006. Growth strata and their application in timing deformation of foreland thrust-fold belts in the north margin of Tianshan. Oil and Gas Geology 27, 475–481 (in Chinese with English abstract).

Guo, Z.J., Wu, C.D., Zhang, Z.C., Chen, W., 2011. Tectonic control on hydrocarbon accumulation and prospect for large oil-gas field exploration in the Southern Junggar Basin. Geological Journal of China Universities 17, 185–195 (in Chinese with English abstract).

Han, B.F., He, G.Q., Wang, X.C., Guo, Z.J., 2011. Late Carboniferous collision between the Tarim and Kazakhstan-Yili terranes in the western segment of the South Tian Shan Orogen, Central Asia, and implications for the Northern Xinjiang, western China. Earth-Science Reviews 109, 74–93.

Hendrix, M.S., Graham, S.A., Carroll, A.R., Sobel, E.R., Mcknight, C.L., Schulein, B.J., Wang, Z.X., 1992. Sedimentary record and climatic implications of recurrent deformation in the Tian Shan: evidence from Mesozoic strata of the North Tarim, South Junggar and Turpan basins, Northwest China. Geological Society of America Bulletin 104, 53–79.

Hendrix, M.S., Dumitru, T.A., Graham, S.A., 1994. Late Oligocene-early Miocene unroofing in the Chinese Tian Shan: an early effect of the India-Asia collision. Geology 22, 487–490.

Hurford, A.J., Green, P.F., 1983. The zeta-age calibration of fission-track dating. Isotope Geoscience 1, 285–317.

Hurford, A.J., 1990. Standardization of fission track dating calibration: recommendation by the Fission Track Working Group of the I.U.G.S. subcommission on geochronology. Chemical Geology 80, 171–178.

Jolivet, M., Brunel, M., Seward, D., Xu, Z., Yang, J., Roger, F., Tapponnier, P., Malavieille, J., Arnaud, N., Wu, C., 2001. Mesozoic and Cenozoic tectonics of the northern edge of the Tibetan plateau: fission-track constraints. Tectonophysics 343, 111–134.

Jolivet, M., Dominguez, S., Charreau, J., Chen, Y., Li, Y.A., Wang, Q.C., 2010. Mesozoic and Cenozoic tectonic history of the central Chinese Tian Shan: reactivated tectonic structures and active deformation. Tectonics 29. http://dx.doi.org/10.1029/2010TC002712.

Ketcham, R.A., 2005. Forward and inverse modeling of low-temperature thermochronometry data. Reviews in Mineralogy and Geochemistry 58, 275–314.

Ketcham, R.A., Carter, A., Donelick, R.A., Barbarand, J., Hurford, A.J., 2007. Improved modeling of fission-track annealing in apatite. American Mineralogist 92, 799–810.

Li, J.Y., 2004. Late Neoproterozoic and Paleozoic tetonic framework and evolution of Eastern Xinjiang, NW China. Geological Review 50, 304–322 (in Chinese with English abstract).

Li, T., Wang, Z.X., Zhou, G.Z., Liu, Y.Q., Li, Y., 2004. The segmentation and the relationship between shallow and deep structure of Bogda Mountain, Xinjiang, Northwest China. Earth Science Frontiers 11, 103–114 (in Chinese with English abstract).

Li, J.F., Tang, W.H., Liu, Z., Zhang, Z.C., 2010. Apatite fission track analysis of Upper Jurassic Houcheng Formation at Qianjiadian area, Beijing and its geological significance. Chinese Journal of Geophysics 53, 2907–2917 (in Chinese with English abstract).

Li, Q., Chen, X., Liu, Y., Bao, A.M., Veroustraete, F., 2012. Regional evapotranspiration retrieval in arid areas. Journal of Arid Land Resources and Environment 26, 108–112 (in Chinese with English abstract).

Li, Z., Peng, S.T., 2013. U-Pb geochronological records and provenance system analysis of the Mesozoic-Cenozoic sandstone detrital zircons in the northern and southern piedmonts of Tianshan, Northwest China: responses to intracontinental basin-range evolution. Acta Petrologica Sinica 29, 739–755 (in Chinese with English abstract).

Liu, Y.Q., Wang, Z.X., Jin, X.C., Li, T., Li, Y., 2004. Evolution, chronology and depositional effect of uplifting in the eastern sector of the Tianshan Mountains. Acta Geological Sinica 78, 319–331 (in Chinese with English abstract).

Ma, R.S., Wang, X.Y., Ye, S.F., 1993. Tectonic Framework and Crustal Evolution of Eastern Tianshan Mountains. Publishing House of Nanjing University, Nanjing, pp. 15–18 (in Chinese).

McDowell, F.W., McIntosh, W.C., Farley, K.A., 2005. A precise $^{40}Ar/^{39}Ar$ reference age for the Durango apatite (U-Th)/He and fission-track dating standard. Chemical Geology 214, 249–263.

Molnar, P., Tapponnier, P., 1975. Cenozoic tectonics of Asia-effects of a continental collision. Science 189, 419–426.

Naeser, C.W., Cebula, G.T., 1985. Re-collection of fish canyon tuff for fission-track standardization. Nuclear Tracks and Radiation Measurements 10, 393.

Pan, C.C., Zhou, Z.Y., Fan, S.F., Xie, Q.L., Wang, X.L., Wang, Y.T., 1997. Thermal history of Junggar Basin. Geochimica 26, 1–7 (in Chinese with English abstract).

Qiu, N.S., Yang, H.B., Wang, X.L., 2002. Tectono-thermal evolution in the Junggar Basin. Chinese Journal of Geology 37, 423–429 (in Chinese with English abstract).

Sengör, A.M.C., Natal'in, B.A., Burtman, V.S., 1993. Evolution of the Altaid tectonic collage and Paleozoic crustal growth in Eurasia. Nature 364, 299–307.

Shen, C.B., Mei, L.F., Liu, L., Tang, J.G., Zhou, F., 2005. Characteristics of fission track age of Bogedashan in Xinjiang and its structural significance. Journal of Oil and Gas Technology 27, 273–276 (in Chinese with English abstract).

Shen, C.B., Mei, L.F., Zhang, S.W., Liu, L., Tang, J.G., Zhou, F., Yan, S.L., Luo, J.C., 2008. Fission-track dating evidence on space-time difference of Mesozoic- Cenozoic uplift of the Yilianhabierga Mountain and Bogda Mountain. Journal of Mineralogy and Petrology 28, 63–70 (in Chinese with English abstract).

Sobel, E.R., Dumitru, T.A., 1997. Thrusting and exhumation around the margins of the western Tarim basin during the India-Asia collision. Journal of Geophysical Research-Solid Earth 102, 5043–5506.

Tapponnier, P., Molnar, P., 1979. Active faulting and Cenozoic tectonics of the Tien Shan, Mongolia, and Baykal regions. Journal of Geophysical Research 84, 3425–3459.

Wang, X.W., Wang, X.W., Ma, Y.S., 2007a. Differential exhumation history of Bogda Mountain, Xinjiang, Northwestern China since the Late Mesozoic. Acta Geological Sinica 81, 1507–1517 (in Chinese with English abstract).

Wang, X.W., Wang, X.W., Ma, Y.S., 2007b. The tectonic evolution of Bogda Mountain, Xinjiang, Northwest China and its relationship to oil and gas accumulation. Geoscience 21, 116–124 (in Chinese with English abstract).

Wang, S.E., Gao, L.J., 2012. SHRIMP U-Pb dating of zircons from tuff of Jurassic Qigu Formation in Junggar Basin, Xinjiang. Geological Bulletin of China 31, 503–509 (in Chinese with English abstract).

Wang, S.E., Pang, Q.Q., Wang, D.N., 2012. New advances in the study of Jurassic-Cretaceous biostratigraphy and isotopic ages of the Junggar Basin in Xinjiang and their significance. Geological Bulletin of China 31, 493–502 (in Chinese with English abstract).

Wang, Z.X., Li, T., Zhang, J., Liu, Y.Q., Ma, Z.J., 2008. The uplifting process of the Bogda Mountain during the Cenozoic and its tectonic implication. Science in China Series D: Earth Sciences 51, 579–593.

Wang, Z.X., Li, T., Zhou, G.Z., Lu, M.A., Liu, Y.Q., Li, Y., 2003. Geological record of the Late-Carboniferous orogeny in Bogdashan, Northern Tianshan Mountains, Northwest China. Earth Science Frontiers 10, 63–69 (in Chinese with English abstract).

Wu, C.D., Guo, Z.J., Fang, S.H., Zhang, Z.C., 2006. The Mesozoic filling sequences and controlling factors in the southern Junggar Basin. In: Guo, Z.J.Z., Chen, L., Shu, L.S.S., Li, X. (Eds.), Mesozoic-Cenozoic intercontinental orogeny and mineralization of the sandstone-type uranium deposit in the Central Asian Orogenic Belt, Northwest China. Geological Publishing House, Beijing, pp. 80–94 (in Chinese with English abstract).

Xiang, C.F., Pang, X.Q., Danisik, M., 2013. Post-Triassic thermal history of the Tazhong Uplift Zone in the Tarim Basin, Northwest China: evidence from apatite fission-track thermochronology. Geoscience Frontiers 4, 743–754.

Xiao, W.J., Windley, B.F., Allen, M.B., Han, C.M., 2012. Paleozoic multiple accretionary and collisional tectonics of the Chinese Tianshan orogenic collage. Gondwana Research 23, 1316–1341.

Yang, S.F., Chen, H.L., Cheng, X.G., Xiao, A.C., Zhou, Y.Z., Lu, H.F., Jia, C.Z., Wei, G.Q., 2003. Cenozoic uplifting and unroofing of Southern Tien Shan, China. Journal of Nanjing University (Natural Sciences) 39, 1–8 (in Chinese with English abstract).

Yang, W., Jolivet, M., Dupont-Nivet, G., Guo, Z.J., Zhang, Z.C., Wu, C.D., 2013. Source to sink relations between the Tian Shan and Junggar Basin (northwest China) from Late Palaeozoic to Quaternary: evidence from detrital U-Pb zircon geochronology. Basin Research 25, 219–240.

Yin, A., 2010. Cenozoic tectonic evolution of Asia: a preliminary synthesis. Tectonophysics 488, 193–325.

Zhang, C.H., Liu, D.B., Zhang, C.L., Wang, Z.Q., Yu, Q.X., 2005. Stratigraphic constraints on the initial uplift age of Bogda Shan, Xinjiang, northwest China. Earth Science Frontiers 12, 294–302 (in Chinese with English abstract).

Zhang, L.C., Wu, N.Y., 1985. The geotectonic and its evolution of Tianshan. Xinjiang Geology 3, 1–14 (in Chinese with English abstract).

Zhang, Z.C., Wang, X.S., 2004. The issues of application for the fission track dating and its geological significance. Acta Scientiarum Naturalium Universitatis Pekinensis 40, 898–905 (in Chinese with English abstract).

Zhang, Z.C., Guo, Z.J., Wu, C.D., Fang, S.H., 2007. Thermal history of the Jurassic strata in the Northern Tianshan and its geological significance, revealed by apatite fission-track and vitrinite-reflectance analysis. Acta Petrologica Sinica 23, 1683–1695 (in Chinese with English abstract).

Zhu, W.B., Shu, L.S., Wang, J.L., Sun, Y., Wang, F., Zhao, Z.Y., 2006. Fission-track evidence for the exhumation history of Bogda-Harlik Mountain, Xinjiang since the Cretaceous. Acta Geological Sinica 80, 16–22 (in Chinese with English abstract).